JOURNAL OF AGRICULTURAL AND FOOD CHEMISTRY

NOTTINGHAM TRENT UNIVERSITY

Subscriber access provided by Nottingham Trent University

Functional Structure/Activity Relationships

Modification, antitumor activity and targeted PPAR# study of 18#-glycyrrhetinic acid, an important active ingredient of licorice

Juan Sun, Han-Yu Liu, Cheng-Zhi Lv, Jie Qin, and Yuanfeng Wu

J. Agric. Food Chem., **Just Accepted Manuscript** • DOI: 10.1021/acs.jafc.9b03442 • Publication Date (Web): 07 Aug 2019

Downloaded from pubs.acs.org on August 10, 2019

Just Accepted

"Just Accepted" manuscripts have been peer-reviewed and accepted for publication. They are posted online prior to technical editing, formatting for publication and author proofing. The American Chemical Society provides "Just Accepted" as a service to the research community to expedite the dissemination of scientific material as soon as possible after acceptance. "Just Accepted" manuscripts appear in full in PDF format accompanied by an HTML abstract. "Just Accepted" manuscripts have been fully peer reviewed, but should not be considered the official version of record. They are citable by the Digital Object Identifier (DOI®). "Just Accepted" is an optional service offered to authors. Therefore, the "Just Accepted" Web site may not include all articles that will be published in the journal. After a manuscript is technically edited and formatted, it will be removed from the "Just Accepted" Web site and published as an ASAP article. Note that technical editing may introduce minor changes to the manuscript text and/or graphics which could affect content, and all legal disclaimers and ethical guidelines that apply to the journal pertain. ACS cannot be held responsible for errors or consequences arising from the use of information contained in these "Just Accepted" manuscripts.

is published by the American Chemical Society. 1155 Sixteenth Street N.W., Washington, DC 20036

Published by American Chemical Society. Copyright © American Chemical Society. However, no copyright claim is made to original U.S. Government works, or works produced by employees of any Commonwealth realm Crown government in the course of their duties.

Modification, antitumor activity and targeted PPARγ study of 18β-glycyrrhetinic acid, an important active ingredient of licorice

Juan Sun[1,3], Han-Yu Liu[2], Cheng-Zhi Lv[1], Jie Qin[2], Yuan-Feng Wu*[1]

[1]School of Biological & Chemical Engineering, Zhejiang University of Science & Technology, Hangzhou 310023, PR China

[2]School of Life Science, Shandong University of Technology, Zibo 255049, PR China

[3] Elion Nature Biological Technology Co., Ltd, Nanjing 210046, PR China

ABSTRACT: Licorice is a traditional Chinese medicine, which is often used as sweetener and cosmetic ingredients in food and pharmaceutical industries. Among them, glycyrrhetic acid is one of the most important agents. Studies have shown that glycyrrhetic acid exhibited anti-tumor activities as PPARγ agonist. However, the limited number of PPARγ glycyrrhetinic agonists and their high toxicity greatly limit the design based on the structure. Therefore, clarifying the binding mode between PPARγ and small molecules, we focused on the introduction of natural active piperazine skeleton in the position of glycyrrhetinic acid C-3. According to the Combination Principle and the Structure-Based Drug Design, nineteen glycyrrhetic acid derivatives were designed and synthesized as potential PPARγ agonists. Compounds **4c** and **4q** were screened as high-efficiency and low-toxic lead compounds.

KEYWORDS: glycyrrhetic acid, molecular docking, piperazine, antitumor, PPARγ

23 **INTRODUCTION**

24 Among traditional Chinese medicines, licorice is a common medicinal plant and
25 is often used as a sweetener and cosmetic ingredient in the food and pharmaceutical
26 industries. Glycyrrhetinic acid is a class of pentacyclic triterpenoids extracted from
27 the roots of licorice, which is a component that actually exerts biological activity
28 through metabolism after taking licorice[1]. Studies have found that glycyrrhetinic acid
29 has a variety of pharmacological activities, such as anti-tumor, anti-inflammatory,
30 anti-ulcer, hypoglycemic and liver protection[2-7]. There are two isomers of
31 glycyrrhetinic acid (Figure 1), of which 18β-glycyrrhetinic acid is the main form.

32 At present, pharmacists have synthesized more than 400 glycyrrhetinic acid
33 derivatives related to cancer cytotoxic, of which nearly 130 compounds exhibit
34 anti-tumor activity with IC_{50} value less than 30 μM[8]. According to analyze the activity
35 data and mechanism, we found that glycyrrhetinic acid and its derivatives can mediate
36 the expression of many key factors in cancer cell lines and have anti-proliferation /
37 apoptosis and/or anti-invasion / anti-metastasis activities. For example, it can reduce
38 the expression of some apoptosis-related proteins, such as Bcl-2 and Bax. Besides, it
39 could affect the expression of MMP-2/MMP-9 and other cell migration-related
40 proteins[9-12]. Studies on pro-apoptosis of glycyrrhetinic acid and chemoprevention of
41 cancer have shown that glycyrrhetinic acid can reduce tumor cell migration ability
42 and induce tumor cell apoptosis by activating Peroxisome proliferator-activated
43 receptor γ (PPARγ), and has been verified in various tumor cell lines[13]. PPARγ, a
44 nuclear receptor and transcription factor that regulates the expression of many genes

relevant to carcinogenesis, is now an important target for development of new drugs for the prevention and treatment of cancer[14-16].

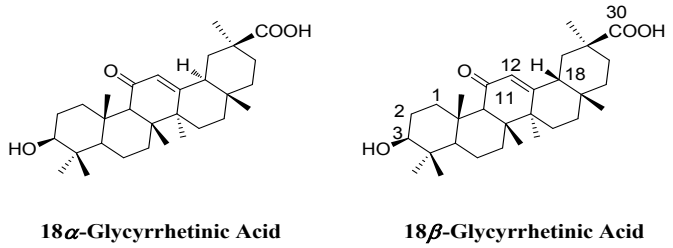

Figure 1. 18-α and 18-β-Glycyrrhetinic Acid

The major challenge of cancer-related death is due to tumor metastasis and multidrug resistance. The natural products of glycyrrhetinic acid targeting PPARγ may offer hope in combating cancer types associated with poor prognoses. Stephen Safe[17-18] reported that 2-cyano substituted analogues of glycyrrhetinic acid (Figure 2, **1, 2**) could inhibit HT-29 and HCT-15 colon cancer cells as PPARγ agonists. Robert Kiss[19] discovered that glycyrrhetinic acid derivative (Figure 2, **3**) displayed similar efficiency in apoptosis-sensitive versus apoptosis-resistant cancer cell lines. The structural modification of glycyrrhetinic acid and its derivatives against PPARγ has shown some activity, but there are still some shortcomings. The mechanism of action is not clear, and the toxicity of derivatives has not been further improved. According to the data analysis of structure-activity relationship, it is found that the formation of double bonds at C1-C2 site and the introduction of electronegative functional groups at C2 site can improve cytotoxicity. In addition, the formation of short alkyl esters from C30 carboxyl group and the oxidation of C3 hydroxyl group or the introduction of ester group and diamino group can significantly improve the cytotoxicity[2]. Therefore, in this manuscript, nineteen glycyrrhetic acid derivatives were designed

and synthesized as potential PPARγ agonists, according to the Combination Principle and the Structure-Based Drug Design.

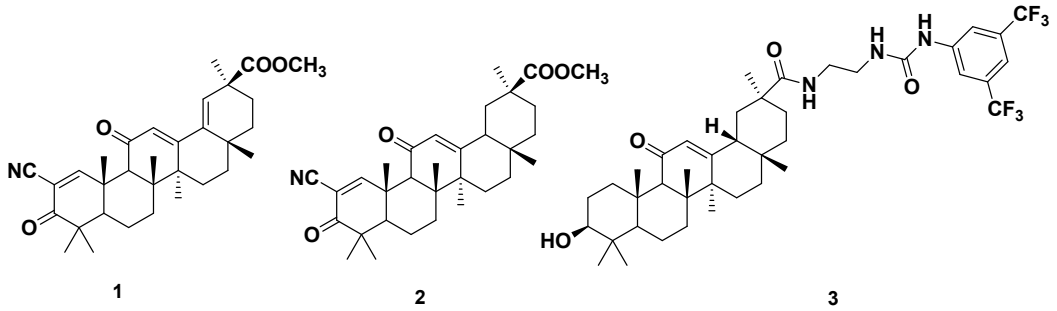

Figure 2. Glycyrrhetinic acid derivatives as PPARγ agonists.

MATERIALS AND METHODS

Materials. All chemicals (reagent grade) used were purchased from either Aladdin (Shanghai, China) or Sangon Biotech. All the ^{1}H NMR and ^{13}C NMR spectra were recorded on a Bruker DPX 400 model spectrometer in $CDCl_3$, and chemical shifts (d) are reported as parts per million (ppm). Melting points were determined on a Digital Melting Point apparatus (Shenguang., Shanghai, China). Thin layer chromatography (TLC) was performed on silica gel plates (Silica Gel 60 GF254) and visualized in UV light (254 nm and 365 nm). The PPARγ Kinase Assay Kit was purchased from Jiangsu Jingmei Biotechnology Co., Ltd. Human hepatoma cell line (HepG2), human breast cell line (MCF-7) and Mouse fibroblast (L929) were purchased from Nanjing Keygen Technology (Nanjing, China).

General procedure for the synthesis of compounds 4a-4s. The synthetic route of target compounds (**4a-4s**) is shown in Scheme 1.

18-β glycyrrhetic acid (1g) and concentrated sulfuric acid (0.5 mL) was dissolved in methanol (30 mL) and refluxed for 24 h while monitoring by TLC. The

89 reaction mixture was concentrated under reduced pressure and extracted with ethyl
90 acetate and water (1:3). The organic layer was collected, dried over anhydrous sodium
91 sulfate, and the solvent was evaporated under reduced pressure to give a crude
92 product which was recrystallized from ethanol to give a pure compound **2**.

93 Bromoacetyl bromide (10 mmol) was slowly added to a solution of compound **2**
94 (10 mmol) in anhydrous dichloromethane (30 mL) and the mixture was stirred at
95 room temperature for 3 h while monitoring by TLC. The mixture was then
96 concentrated under reduced pressure and extracted with ethyl acetate and saturated
97 aqueous solution of $NaHCO_3$ (1:3). The organic layer was collected, dried over
98 anhydrous sodium sulfate, and the solvent was evaporated under reduced pressure to
99 give a crude product which was recrystallized from acetone to give the pure
100 compound **3**.

101 The compound **3** (1mmol) and different substituted piperazines (1mmol) were
102 dissolved in acetonitrile, then the potassium carbonate (3 mmol) was added and the
103 reaction was refluxed for 8 hours in 85°C. After the reaction was completed, the
104 reaction solution was evaporated to dryness under reduced pressure, extracted with
105 ethyl acetate and water (3:1), the organic layer was dried over anhydrous sodium
106 sulfate, and the solvent was evaporated under reduced pressure to give the crude
107 product as acetone. Compounds **4a-4s** were recrystallized with acetone. The ^{1}H NMR
108 and ^{13}C NMR spectra data was described in Materials and Methods.

109

110

Scheme 1. General procedure for the synthesis of compounds **4a-4s.**

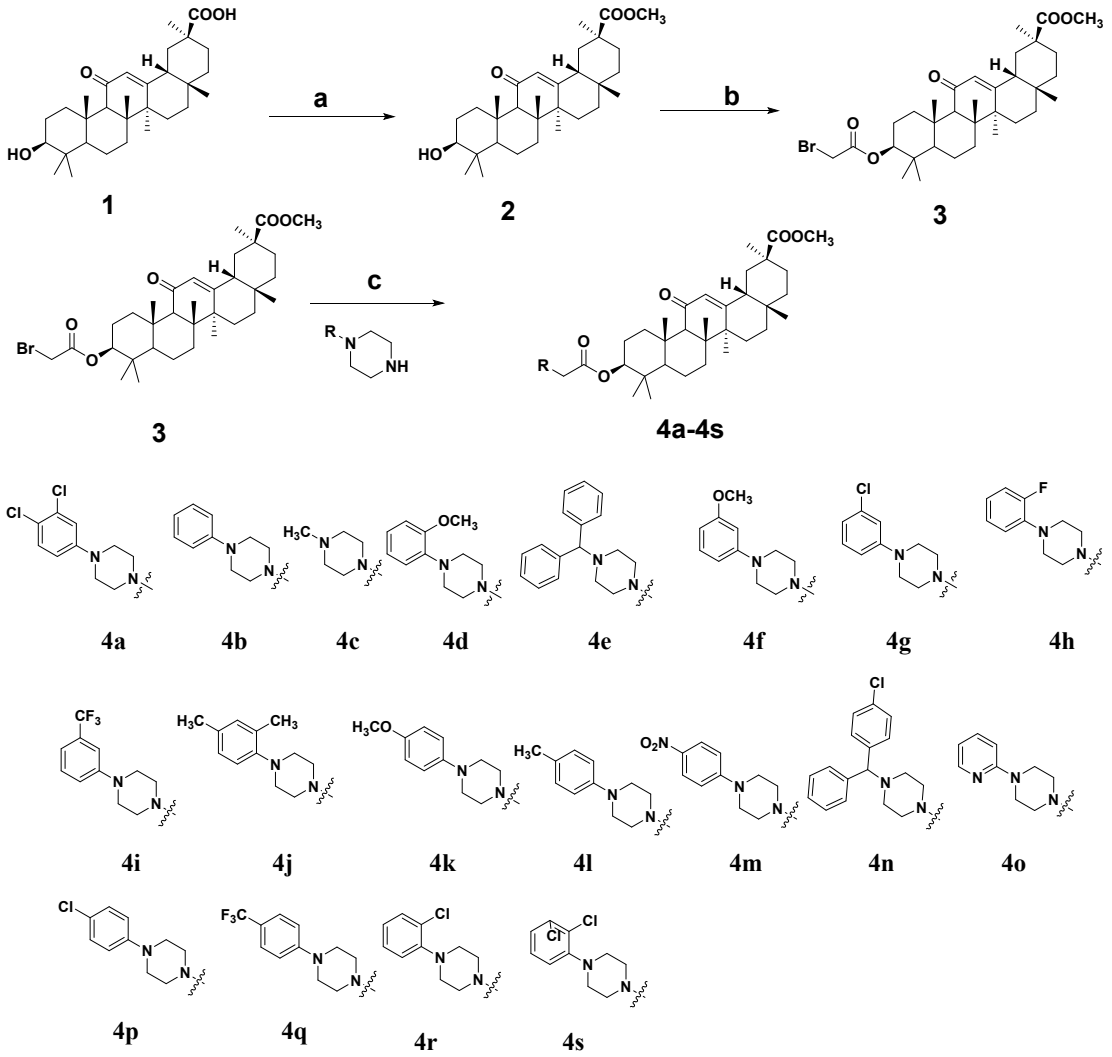

Reagents and conditions: (a) Concentrated sulfuric acid, CH_3OH, reflux; (b) Bromoacetyl bromide, CH_2Cl_2, rt; (c) Different substituted piperazines, K_2CO_3, Acetonitrile, reflux.

X-ray crystallography. Single crystal X-ray diffraction data was collected on a Bruker *D-8* venture diffractometer at room temperature (293 K). The X- ray generator was operated at 50 kV and 35 mA using Mo Kα radiation (k = 0.71073 Å). The data was collected using SMART software package. The data were reduced by SAINT-PLUS, an empirical absorption correction was applied using the package SADABS and XPREP were used to determine the space group. The crystal structure

123 was solved by direct methods using SIR92 and refined by full-matrix least-squares
124 method using SHELXL97 [20-21]. All non-hydrogen atoms were refined anisotropically
125 and hydrogen atoms have been refined in the riding mode on their carrier atoms
126 wherever applicable.

127 **Anti-tumor proliferation activity test.** The anticancer activities of the prepared
128 compounds in vitro have been evaluated against MCF-7, HepG2 cell lines. Target
129 tumor cells were cultured in Dulbecco's modified Eagle's medium (DMEM, Hyclone)
130 (High Glucose) medium supplemented with 10% fetal bovine serum (FBS). After
131 reaching a dilution of 1×10^5 cells mL^{-1} with the medium, 100 μL of the obtained cell
132 suspension was added to each well of 96-well culture plates. Subsequently, incubation
133 was performed at 37 ℃ in 5% CO_2 atmosphere for 4h. Tested samples at preset
134 concentrations were added to 6 wells with 5-Fluorouracil being employed as a
135 positive reference. After 24 h exposure period, 25 μL of PBS containing 4 mg • mL^{-1}
136 of MTT was added to each well. After 4 h, the medium was replaced by 150 μL
137 DMSO to dissolve the purple formazan crystals produced. The absorbance at 570 nm
138 of each well was measured with an ELISA plate reader. The data represented the
139 mean of three independent experiments in triplicate and were expressed as means ±
140 SD. The IC_{50} value was defined as the concentration at which 50% of the cells could
141 survive.

142 **PPARγ agonistic activity test.** The PPARγ Enzyme-linked Immunoassay Kit
143 was used to test PPARγ agonistic activities. The experiments were performed
144 according to the manufacturer's instructions.

145 **Wound healing assay.** The MCF-7 cancer cells at a density of 2×10^5 were
146 seeded into 6-well plates and allowed to attain confluent monolayers. In the center of
147 each well a line was drawn using a 200 ml pipette tip for producing wound area. The
148 cells were washed with PBS two times to remove the non-adherent cells. Various con-
149 centration of Compound **4q** were added to each of the well in medium containing 1%
150 FBS. The cells were then cultured for 24 h in FBS free DMEM medium. Images were
151 captured at a magnification of ×100 using a fluorescence inverted microscope at 0
152 hours and 24 hours, respectively. Finally, Image J was used for image processing and
153 data acquisition.

154 **Western Blot analysis.** Protein extracts (50 μg) prepared with RIPA lysis buffer
155 [50 mM Tris-HCl, 150 mM NaCl, 0.1% sodium dodecyl sulfate (SDS), 1% NP-40,
156 0.5% sodium deoxy- cholate, 1 mM phenylmethylsulfonyl fluoride (PMSF), 100 μM
157 leupeptin, and 2 μg /mL aprotinin (pH 8.0)] were separated on an 10% or 12%
158 SDS-polyacrylamide gel and transferred to PVDF membranes. The membranes were
159 stained with 0.2% Ponceau S red to assure equal protein loading and transfer. After
160 blocking with 5% nonfat milk, the membranes were incubated with a specific
161 antibody to PARP, Cleaved-PARP, MMP-2, MMP-9, PPARγ or β-actin overnight at
162 4°C. Immunocomplexes were visualized using enhanced chemiluminescence Western
163 blotting detection reagents (Amersham Biosciences, England, UK). Protein
164 quantitation was determined by the BCA (Bicinchoninic acid) Protein Concentration
165 Quantification Kit.

166 **Cell apoptosis assay.** Approximately 10^5 cells/well were plated in a 24-well

167 plate and allowed to adhere. Subsequently, the medium was replaced with fresh
168 culture medium containing compound **4q** at final concentrations of 0, 6.25, 12.5 and
169 25 μM. Non-treated wells received an equivalent volume of ethanol (<0.1%). After 24
170 h, cells were trypsinized, washed in PBS and centrifuged at 2000 rpm for 5 min. The
171 pellet was resuspended in 500 μL staining solution (containing 5 μL AnnexinV-FITC
172 and 5 μL PI in Binding Buffer), mixed gently and incubated for 15 min at room
173 temperature in dark. The samples were then analyzed by a FACSCalibur flow
174 cytometer (Becton Dickinson, San Jose, CA, USA)

175 **Molecular docking study.** Molecular docking of compounds into the three
176 dimensional X-ray structure of PPARγ (PDB code: 2HFP) was carried out using the
177 Discovery Studio (version 4.5) as implemented through the graphical user interface
178 DS-CDOCKER protocol. The 3D structure of EGFR (2HFP) in docking study was
179 downloaded from Protein Data Bank. The three-dimensional structures of the
180 aforementioned compounds were constructed using Chem. 3D ultra 12.0 software
181 [Chemical Structure Drawing Standard; Cambridge Soft corporation, USA (2010)],
182 then they were energetically minimized by using MMFF94 with 5000 iterations and
183 minimum RMS gradient of 0.10. All bound waters and ligands were eliminated from
184 the protein and the polar hydrogen was added to the proteins. Each compound would
185 retain 10 poses, and were ranked by CDOCKER_INTERACTION_ENERGY.
186 Docking algorithm utilized: CDOCKER algorithm; definition of binding site: 25.432,
187 -7.312, 2.931; radius: 15 Å; scoring function: CDocker interaction energy; rigid
188 receptor: PDB code 2HFP; flexible ligand docking: YES; cluster analysis of docking

189 poses: ten optimal poses were retained.

190 **Statistical analysis.** All experiments were performed in triplicate. The data
191 presented are the mean of ±SD and were analyzed using SPSS software, version 16.0
192 (SPSS, Inc., Chicago, IL, USA). $P < 0.05$ was considered to indicate a statistically
193 significant difference.

194

195 **RESULTS AND DISCUSSION**

196 **Structure-based design of small molecules**. Rosiglitazone, a thiazolidinedione
197 derivative, has been proved to be one of the classical PPAR*γ* agonists [22]. As shown in
198 Figure 3A and 3B, when rosiglitazone binds to the LDB of PPAR*γ*, it interacts with
199 HIS323, TYR473 and HIS449 in the AF-2 domain, resulting in the formation of
200 hydrophobic ditches, which fold helical H12 along the core of LBD with helical H3
201 and H5 to form a more compact and rigid conformation. This conformational change
202 can lead to the recruitment of various cofactors required for gene transcription [23]. We
203 found that four amino acid residues (HIS322, HIS449, LYS457, TYR473) are key
204 amino acid residues with high affinity to PPAR*γ* (Figure 3C and 3D) [24]. Therefore,
205 based on the basic skeleton of glycyrrhetinic acid, we have selected phenyl piperazine
206 skeleton at the C3 position. It can effectively bind to the active pocket confinement
207 cavity formed by PPAR*γ* H12 helix and act as an "anchor" to anchor the molecule on
208 PPAR*γ*. Besides, the main skeleton of glycyrrhetinic acid is located near the opening
209 of the confinement chamber, which can form a strong hydrogen bond to enhance the
210 stability of the binding of small molecules to PPAR*γ*. At the same time, The C30

211 group of glycyrrhetinic acid can be extended to the back of the H12 spiral
212 confinement chamber after being replaced by methyl ester, further enhancing the
213 affinity with PPARγ (Figure 3E)..

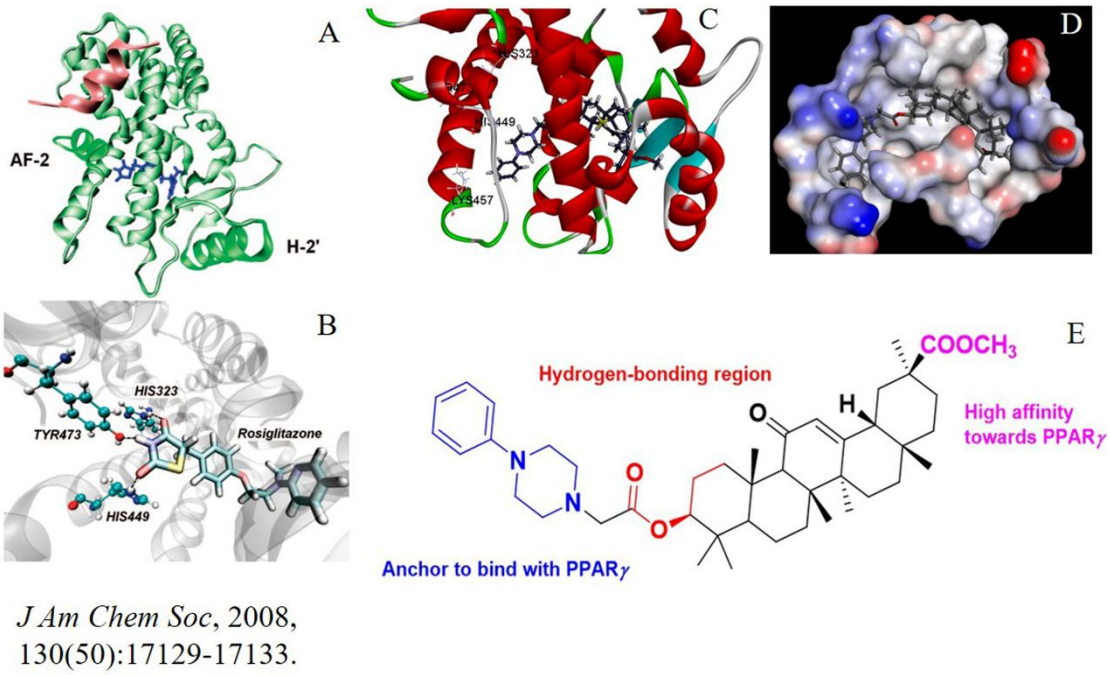

214

215 Figure 3. Simulated interaction between target compounds and PPARγ.

216 **Chemistry.** The synthesis of twenty 18-β glycyrrhetic acid derivatives **(4a-4s)**
217 followed the general pathway outlined in Scheme 1. The newly synthesized
218 compounds were characterized ^{1}H NMR and ^{13}C NMR analysis. The spectral data of
219 newly synthesized compounds **4a-4s** are provided in the supporting information, and
220 in accordance with the assigned structures of the compounds. All of the synthetic
221 compounds gave satisfactory analytical and spectroscopic data, which were full
222 accordance with their depicted structures.

223 **Crystal structure of compound 4h.** Crystals of compound **4h** were obtained
224 from Acetone solution. Figure 4 shows a perspective view of the monomeric unit with
225 the atomic numbering scheme, and Figure 5 depicts the Two-dimensional stacked

226 graph. Crystallographic data, details of data collection and structure refinement
227 parameters are listed in Table 1. A single crystal of compound **4h** (0.15 mm × 0.15
228 mm × 0.12 mm) was measured under a condition of 296 K using a *D-8* VENTURE
229 single crystal ray diffractometer of a graphite monochromator MoKa having a λ value
230 of 0.71073 Å. A total of 37776 diffracts were collected for compound **4h**, where
231 14095 was R_{int} = 0.176. The last round of the refined full-matrix least squares method
232 converges to the values of R and *w*R of 0.4809 and 0.3344, respectively. The
233 maximum peaks and valleys on the difference Fourier map are 0.29 and -0.28 e $Å^{-3}$,
234 respectively.

235 **Table 1.** Crystallographic data, details of data collection and structure refinement parameters.

Crystal	Compound **4h**
Empirical formula	$C_{43}H_{61}FN_2O_5$
Formula mass	704.94
Color, habit	Colorless, block
Crystal dimensions (mm)	0.15 x 0.15 x 0.12
Crystal system	Triclinic
Space group	*P1*
Z	2
a (Å)	7.521(2)
b (Å)	11.316(3)
c (Å)	23.122(7)
α(°)	90.00
β(°)	82.181(6)
γ(°)	90.00
Collection ranges	$-9 \leq h \leq 8$, $-15 \leq k \leq 14$, $-30 \leq l \leq 30$
Temperature (K)	296

Volume(Å^3)	1949.5(9)
D_{calcd} (Mg m^{-3})	1.201
Radiation	Mo Kα (λ = 0.71073)
Absorption coeff. (μ) (mm^{-1})	0.081
Absorption correction	multi-scan
F(000)	764
Θ range for data collection (º)	2.5- 28.4
Observed reflections	37776
Independent reflections	14095 (R_{int} = 0.176)
Data/restraints/parameters	4154/0/ 935
Maximum shift/error	0.00
Goodness-of-fit on F^2	1.112
Final R indices [$I > 2\sigma(I)$]	R_1 = 0.4809, R_2 =0.3344
R indices (all data)	R_1 = 0.2056, R_2 = 0.2354
Absolute structure parameter	N/A
Extinction coefficient	N/A
Largest diff. Peak and hole (e Å^{-3})	0.29 and -0.28

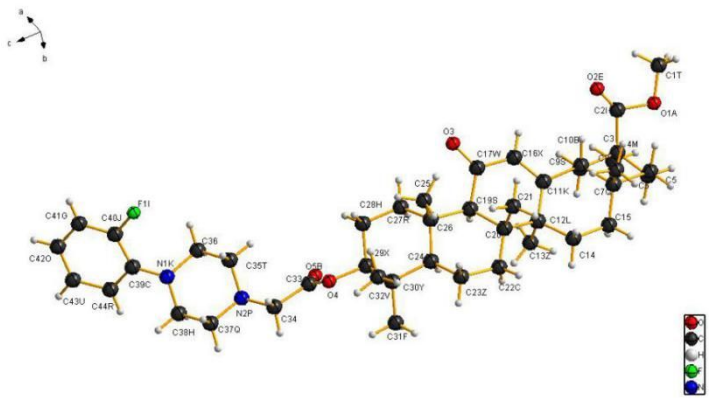

Figure 4. Molecular structures of the compound **4h** with atomic numbering scheme.

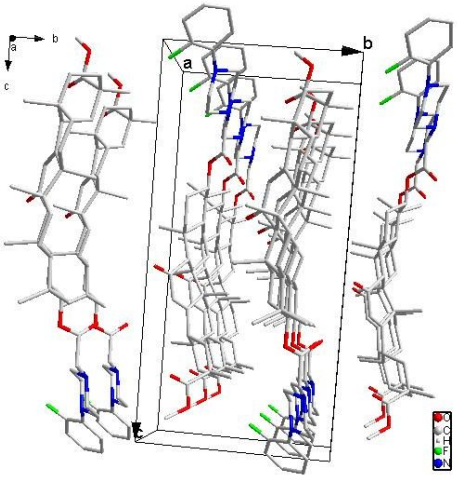

Figure 5. Two-dimensional stacked diagram of compound **4h**.

Anti-tumor cell proliferation and cytotoxicity test. To test the antiproliferative activities and cytotoxicity of the synthesized compounds, the target compounds were evaluated *in vitro* antiproliferation assays against two human cancer cell lines (MCF-7 and HepG2) and mouse fibroblast was evaluated for *in vitro* cytotoxicity. The results were summarized in Table 2.

Table2. *In vitro* anticancer activities (IC_{50} μM) against two human tumor cell lines

Compounds	IC_{50}±SD (μM)		CC_{50}±SD (μM)
	MCF-7	HepG2	L929
4c	6.898±0.839	9.949±0.998	333.885±2.524
4e	31.588±1.500	21.939±1.341	600.657±3.140
4l	16.320±1.213	20.510±1.312	121.488±2.085
4m	18.003±1.255	34.163±1.534	49.965±1.699
4n	34.445±1.537	26.260±1.419	259.131±2.414
4o	11.572±1.063	21.040±1.302	33.671±1.527
4p	8.073±0.907	16.614±1.220	95.230±1.979
4q	9.500±0.978	25.585±1.408	650.226±2.822
G1	29.555±1.471	28.146±1.449	321.630±2.507

G2	60.090±1.779	16.187±1.209	114.385±2.058
Rosiglitazone	38.747±1.781	30.318±1.482	297.589±2.474
5-FU	13.189±1.120	17.373±1.240	339.217±2.530

247 The results showed that all the compounds showed tumor cell proliferation
248 inhibitory activity, and the inhibitory effect on the proliferation activity of MCF-7
249 tumor cells was significantly stronger than that of HepG2 cells. In addition, most of
250 these compounds exhibited better anti-tumor cell proliferation activity than the
251 intermediate product and the classical PPARγ agonist rosiglitazone, suggesting that
252 introduction of the piperazine ring into glycyrrhetinic acid can increase its anti-tumor
253 cell proliferation potency. The target compound **4c** showed optimal tumor cell
254 proliferation inhibitory activity against both MCF-7 and HepG2 cells, and the
255 inhibitory activity against MCF-7 cells was IC_{50} = 6.898 μM, and the inhibitory
256 activity against HepG2 cells was IC_{50} = 9.949 μM. The inhibitory activity of
257 compound **4p** and compound **4q** against MCF-7 tumor cells was second only to
258 compound **4c** (**4p**: IC_{50} = 8.073 μM, **4p**: IC_{50} = 9.500 μM), and both showed superior
259 tumor cell proliferation inhibition activity than HepG2.

260 Structural-Activity relationship analysis showed that the antiproliferative activity
261 of glycyrrhetinic acid was significantly increased when piperazine skeleton was
262 introduced in the position of glycyrrhetinic acid C-3 (compared with G1 and G2).
263 More importantly, the antiproliferative activity of glycyrrhetinic acid was better when
264 there was no or one benzene ring than two benzene rings. Possibly because the size of
265 the two benzene rings was too large to enter the active cavity, thus it affected the
266 affinity of the active site with the target compound. Besides, when the

267 *para*-withdrawn groups were substituted on the benzene rings, the potency activity
268 order was nitro (**4m**) < trifluoromethyl (**4q**) < chlorine (**4p**). Perhaps the excessive
269 electron-withdrawn groups reduced the electron cloud density of benzene rings and
270 prevented them from interacting with corresponding amino acids to form interactions,
271 thus reduced the affinity with active pockets, and ultimately affected the
272 anti-proliferation activities.

273 Cytotoxicity data showed that most of the compounds had less damage to normal
274 cells, indicating a low toxicity of the target compound. Therefore, Compound **4c** and
275 Compound **4q** were screened as highly efficient and low toxicity lead compounds by
276 comparison with antitumor cell proliferation activity data.

277 **PPAR*γ* agonists assay.** In order to verify that the synthetic target compound
278 exerts anti-tumor cell proliferation activity by targeting agonistic PPAR*γ*, we
279 investigated the agonistic effect of some compounds on PPAR*γ*. Rosiglitazone (ROS)
280 is a class of classical PPAR*γ* full agonists that have been shown to play an important
281 role in hypoglycemic and anti-tumor functions as PPAR*γ* agonists. Therefore, this
282 experiment used ROS as a positive control to confirm the agonistic ability of the
283 target compound to PPAR*γ*. The PPAR*γ* enzyme-linked immunosorbent assay kit was
284 used to detect changes in intracellular PPAR*γ* content of selected compounds
285 mediated MCF-7. The results are shown in Figure 6.

286 The three target compounds acted on the cells and caused an increase in
287 intracellular PPAR*γ* content higher than ROS at 62.5 μM and 12.5 μM. The increase
288 in the amount of PPAR*γ* caused by rosiglitazone at 50 μM was higher than compound

289 **4p** and compound **4q**, but lower than compound **4c**. Through data analysis, it can be
290 determined that the target compound acts on the cells and can increase the expression
291 level of PPARγ in the cells.

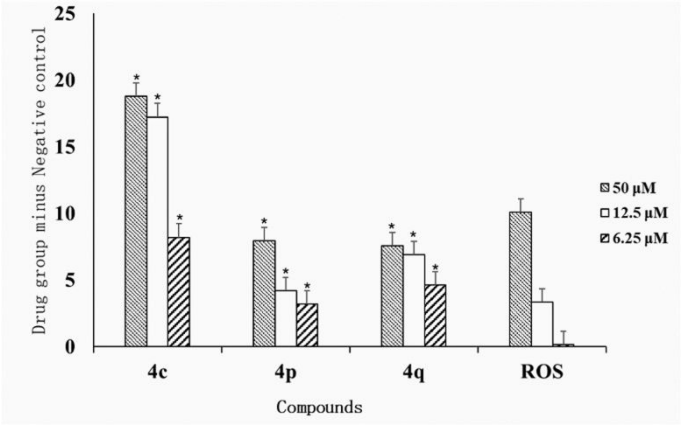

292

293 Figure 6. Targeting PPARγ activity (*: P<0.05, each concentration compared to the positive
294 control)

295 **Western Blot analysis.** To further verify the targeted agonistic activity of the
296 target compound on PPARγ, We used the Western blot assay to demonstrate the
297 targeted agonistic activity of the target compound against PPARγ by detecting the
298 MMP-2/MMP-9 signaling pathway regulated by PPARγ. The results are shown in
299 Figure 7 and Figure 8. Through the analysis of the results, we can find that when
300 compound **4q** acts on MCF-7 cells, it can lead to an increase in PPARγ content and a
301 decrease in MMP-2/MMP-9 content in cells. This indicates that the target compound
302 can reduce the intracellular expression level of MMP2/MMP-9 by activating PPARγ.
303 This experimental data is consistent with the literature report that activation of PPARγ
304 can reduce MMP-2/MMP-9, thus proving the correctness of the results. In addition,
305 MMP-2/MMP-9 is a matrix metalloproteinase, and its reduced intracellular content
306 can attenuate the migration ability of tumor cells. It was also confirmed in the

subsequent tumor cell migration inhibition test.

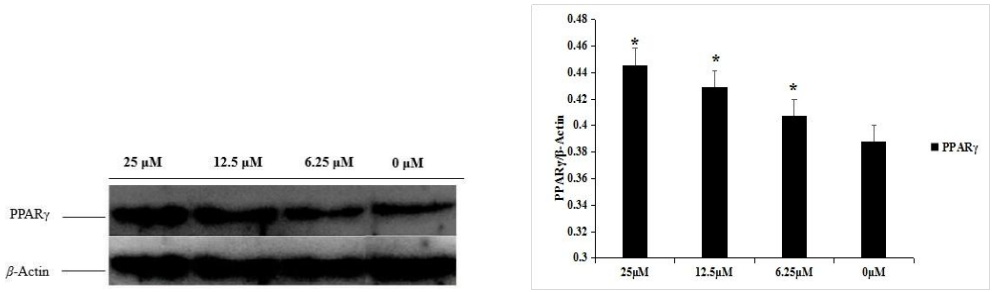

Figure 7. Changes in PPARγ cell expression (*: ***P***<0.05, each concentration compared to the solvent control)

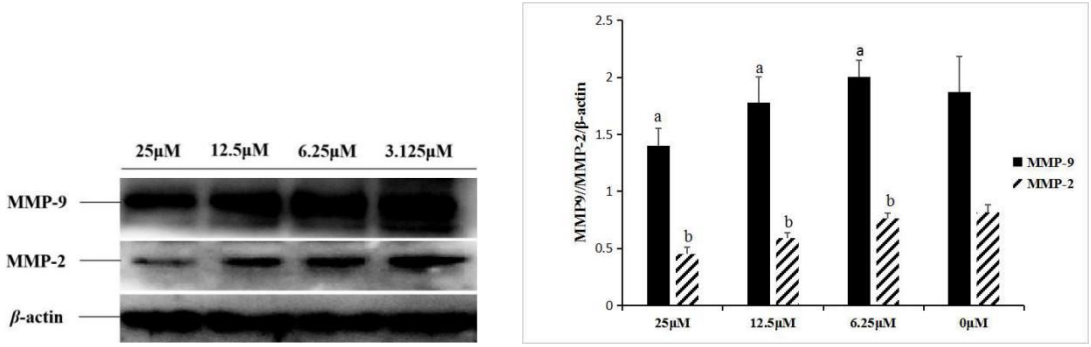

Figure 8. Changes in MMP-2 and MMP-9 cell expression ([a]: *P*<0.05, each concentration of MMP-9 protein was compared with the solvent control, [b]: *P*<0.05, and each concentration of MMP-2 protein was compared with the solvent control)

Tumor cell migration inhibition. Using tumor cell scratch assays, it was verified that the target compound can reduce the migration ability of tumor cells by activating PPARγ. The result is shown on Figure 9. When the compound **4q** was incubated with MCF-7 cells for 24 hours, the percentage of wound healing at 20 μM reached 23%, and the percentage of wound healing at 10 μM reached 35%, whereas the percentage of wound healing of tumor cells without drug action was 51%. The results indicate that compound **4q** can significantly reduce the migration of tumor cell MCF-7. By combining with the previous data, the target compound can activate PPARγ to reduce the migration ability of tumor cells.

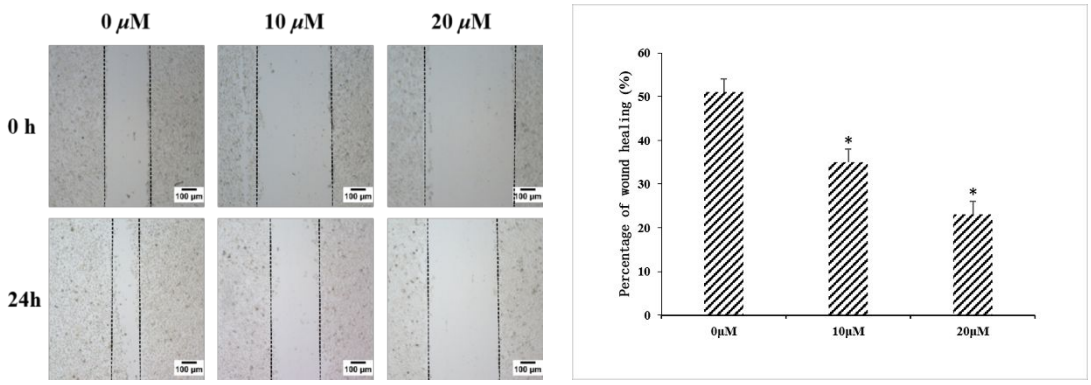

Figure 9. Percentage of wound healing of compound **4q** against MCF-7 cells. (*: ***P***<0.05, each concentration compared to the solvent control)

Apoptosis. Apoptosis is a manifestation of programmed cell death, which is softer than the process of cell death. We envisaged the activation of PPARγ in tumor cells, which enhances the apoptosis of tumor cells and ultimately inhibits tumor cells. The content of the intracellular Cleaved-PARP protein, an apoptotic marker protein, was detected by WB assay after the action of compound **4q** on MCF-7 cells. The result is shown in Figure 10. The results showed that the expression of Cleaved-PARP protein increased in a concentration-dependent manner after the target compound **4q** was applied to MCF-7 cells. This indicates that the target compound can induce apoptosis of tumor cells by activating PPARγ, thereby producing tumor cell inhibitory activity.

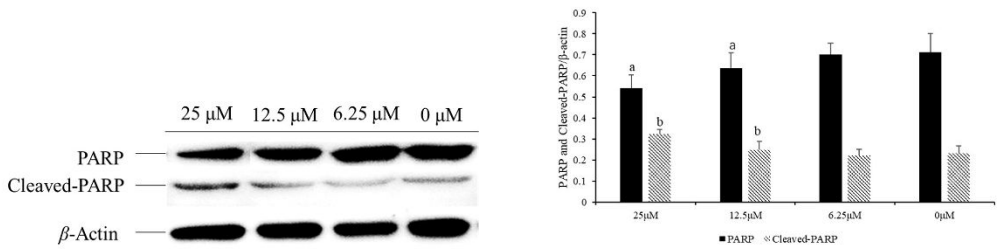

Figure 10. PARP and cleaved-PARP protein cell expression changes (*: $P < 0.05$, protein concentration compared with solvent control)

Besides, we detected the mechanism of compound **4q** inhibition activity by flow

cytometry (FCM) and found that the compound could induce the apoptosis of activated MCF-7cells (Figure 11). As shown in Figure 11, MCF-7 cells were treated with 6.25 μM, 12.5 μM and 25 μM of compound **4q** for 24 h. The compound increased the percentage of apoptosis by Annexin V-FITC/PI staining.

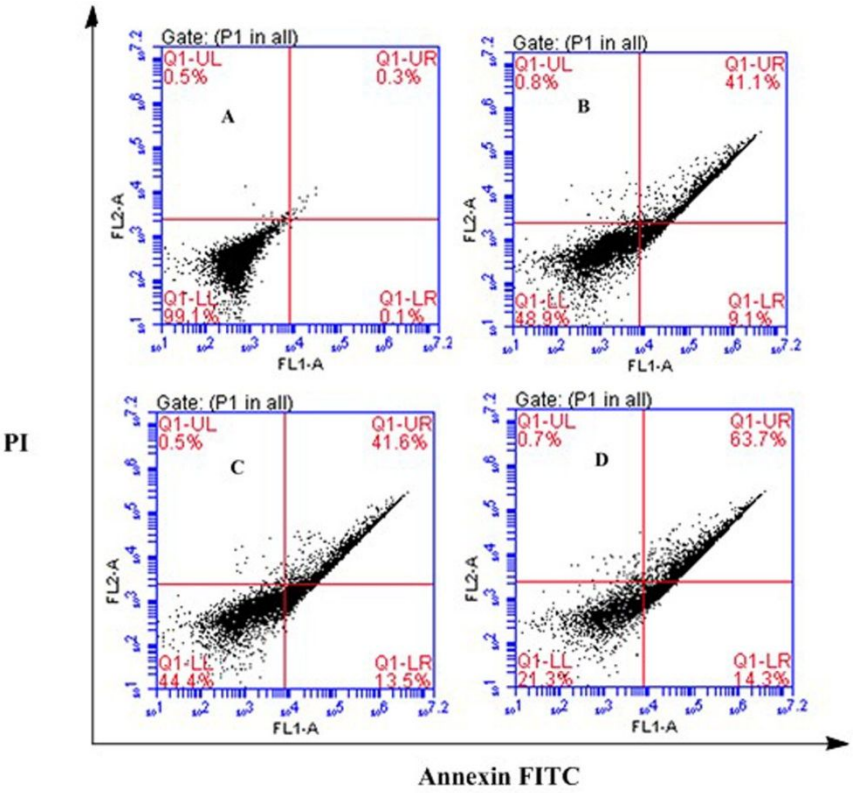

Figure 11. MCF-7 cells were cultured with antitumor and various concentrations of **4q** for 24 h. Cells were stained by Annexin VeFITC/PI and apoptosis was analyzed by flow cytometry. (A) Control. (B) 6.25 μM. (C) 12.5 μM. (D) 25 μM.

Experimental protocol of docking study. Molecular docking of the synthesized compounds and PPARγ was performed on the binding model based on the PPARγ protein complex structure (2HFP.pdb). The docking results of all compounds are shown in Figure 12. The model of compound **4q** docked with PPARγ is depicted in Figure 13.

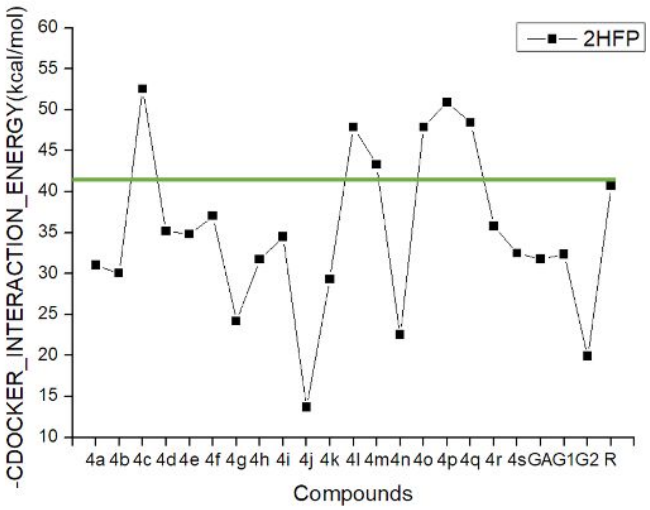

Figure 12. The -CDCKER_INTEACTION_ENERGY (kcal/mol) obtained from the docking study of all synthesized compounds by the CDOCKER protocol.

Analysis of the docking results indicated that compound **4q** was able to bind to the active site and interact with multiple amino acid residues in the active site, thereby increasing the affinity of the compound for PPAR*γ*. Analysis of the docking results indicated that compound **4q** was able to bind to the active site and interact with multiple amino acid residues in the active site, thereby increasing the affinity of the compound for PPAR*γ*. Compound **4q** can form a hydrogen bond interaction with Arg280, Ile281, Ser289 and His323 in the PPAR*γ* site. The phenyl ring of the phenylpiperazine moiety of compound **4q** will form a *Pi-Pi* T-shaped interaction with Phe282.

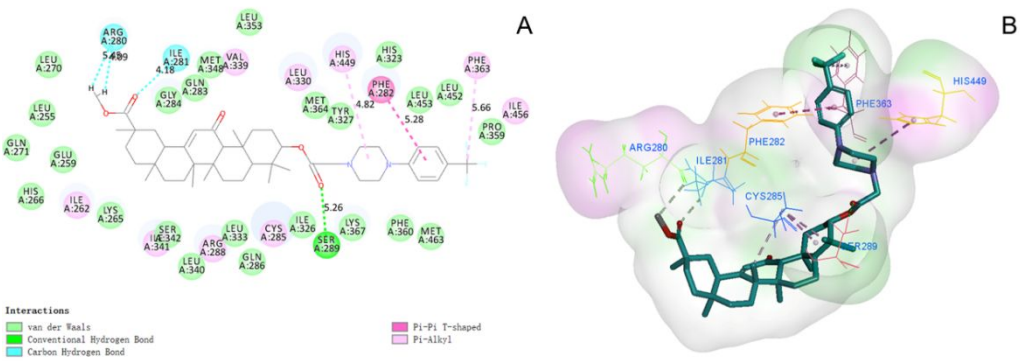

368 Figure 13. Compound **4q** docking model (A) 2D docking diagram; (B) 3D docking diagram

369

370 Licorice is often used as sweetener and cosmetic ingredients in food and
371 pharmaceutical industries. Therefore, it is very important to reconstruct the structure
372 of licorice and find new functions. In our research, PPARγ was used as a drug target,
373 and a series of glycyrrhetic acid derivatives were designed and synthesized by
374 computer simulation drug design technology. The experiment results showed that
375 some compounds exhibited strong antitumor activities, and compounds **4c** and **4q**
376 were screened as high-efficiency and low-toxic lead compounds. We will continue to
377 investigate new licorice derivatives and establish potential functions in our future
378 research.

379

380 **AUTHOR INFORMATION**

381 **Corresponding Author**

382 *Telephone: +86-571-85070383. Fax: +86-571-85070378. Email:
383 sunjuan18@zust.edu.cn

384 **Funding**

385 This work was financially supported by the Shandong Provincial Natural Science
386 Foundation of China (grant no. ZR2018BH040).

387 **Notes**

388 The authors declare no competing financial interest.

389 **ABBREVIATIONS USED**

390 PPARγ, Peroxisome proliferator-activated receptor γ; FBS, Foetal bovine serum;

391 HepG2, Human hepatoma cell line; MCF-7, Human breast cell line; ROS,
392 Rosiglitazone.

393 **REFERENCES**

394 [1] Graebin C S, Verli H, Guimarães J A. Glycyrrhizin and glycyrrhetic acid:
395 scaffolds to promising new pharmacologically active compounds. *J. Brazil. Chem.*
396 *Soc,* 2010, 21(9):1595-1615.

397 [2] Li, B.; Cai, S.; Yang, Y.A; et al. Novel unsaturated glycyrrhetic acids derivatives:
398 Design, synthesis and anti-inflammatory activity. *Eur. J. Med. Chem*., 2017, 139：
399 337-348.

400 [3] Li, B.; Yang, Y A,; Chen, L Z,; et al. 18α-Glycyrrhetinic acid monoglucuronide as
401 an anti-inflammatory agent through suppression of the NF-κB and MAPK signaling
402 pathway. *Med. Chem. Comm*., 2017, 8:1498-1504.

403 [4] Ming, L J.; Yin A C Y. Therapeutic Effects of Glycyrrhizic Acid. *Nat prod*
404 *commun*, 2013, 8(3):415-418.

405 [5] Zong, L.; Qu, Y., Xu, M.Y., et al. 18-alpha-glycyrrhetinic acid down-regulates
406 expression of type I and III collagen via TGF-Beta1/Smad signaling pathway in
407 human and rat hepatic stellate cells. Int. *J. Med. Sci*., 2012, 9(5): 370-379.

408 [6] Shetty, A.V., Thirugnanam, S., Dakshinamoorthy, G., et al.
409 18-alpha-glycyrrhetinic acid targets prostate cancer cells by down-regulating
410 inflammation-related genes. *Int. J. Oncol*., 2011, 39(3): 635-640.

411 [7] Wang, D.; Wong, H.K.; Feng, Y.B.; Zhang, Z. J. 18beta-Glycyrrhetinic acid
412 induces apoptosis in pituitary adenoma cells via ROS/MAPKs-mediated pathway. *J.*

413 *Neurooncol.*, 2014, 116(2): 221-230.

414 [8] Roohbakhsh, A.; Iranshahy， M.; Iranshahi, M. Glycyrrhetinic Acid and Its
415 Derivatives: Anti-Cancer and Cancer Chemopreventive Properties, Mechanisms of
416 Action and Structure-Cytotoxic Activity Relationship. *Curr Med Chem*, 2016, 23:
417 498-517.

418 [9] Satomi, Y.; Nishino, H.; Shibata, S. Glycyrrhetinic acid and related compounds
419 induce G1 arrest and apoptosis in human hepatocellular carcinoma HepG2.
420 *Anticancer Res.,* 2005, *25*(6B), 4043-4047.

421 [10] Wang, D.; Wong, H K.; Feng, Y B.; Zhang, Z J. 18betaGlycyrrhetinic acid
422 induces apoptosis in pituitary adenoma cells *via* ROS/MAPKs-mediated pathway. *J.*
423 *Neurooncol.,* 2014, *116*(2), 221-230.

424 [11] Wang, X F.; Zhou, Q.M.; Lu, Y Y.; et al. Glycyrrhetinic acid potently suppresses
425 breast cancer invasion and metastasis by impairing the p38 MAPK-AP1 signaling
426 axis. *Expert Opin. Ther. Targets,* 2015, *19*(5), 577-587.

427 [12] Yang, J.C.; Myung, S.C.; Kim, W.; Lee, C. S. 18β-Glycyrrhetinic acid
428 potentiates Hsp90 inhibition-induced apoptosis in human epithelial ovarian carcinoma
429 cells *via* activation of death receptor and mitochondrial pathway. *Mol. Cell. Biochem.,*
430 2012, *370*(1-2), 209-219.

431 [13] Ayman M. Mahmoud et al. Methotrexate hepatotoxicity is associated with
432 oxidative stress, and down-regulation of PPARγ and Nrf2: Protective effect of
433 18β-Glycyrrhetinic acid. *Chem-Biol Interact*, 2017, 57: 59-72.

434 [14] Wei-Hsuan Hsu, Bao-Hong Lee, et al. Inhibition of Th2 Cytokine Production in

435 T Cells by Monascin via PPAR-γ Activation. *J Agr Food Chem*, 2013,61:8126-8133.

436 [15] Wei-Hsuan Hsu, Bao-Hong Lee, et al. Monascin Attenuates Oxidative
437 Stress-Mediated Lung Inflammation via Peroxisome Proliferator-Activated
438 Receptor-Gamma (PPAR-*γ*) and Nuclear Factor-Erythroid 2 Related Factor 2 (Nrf-2)
439 Modulation. *J Agr Food Chem*, 2014,62:5337-5344.

440 [16] Wang L, Waltenberger B, Pferschy-Wenzig EM, et al. Natural Product agonists
441 of peroxisome proliferator-activated receptor gamma (PPAR*γ*): a review. *Biochem*
442 *Pharmacol.*, 2014, 92: 73-89.

443 [17] Chintharlapalli S, Papineni S, Jutooru I, et al. Structure-dependent activity of
444 glycyrrhetinic acid derivatives as peroxisome proliferator–activated receptor *γ*
445 agonists in colon cancer cells. *Mol. Cancer. Ther*. 2007, 6(5): 1588-1598.

446 [18] Jutooru I, Chadalapaka G, Chintharlapalli S, et al. Induction of apoptosis and
447 nonsteroidal anti-inflammatory drug‐activated gene 1 in pancreatic cancer cells by a
448 glycyrrhetinic acid derivative. *Mol. carcinogen*. 2009, 48(8): 692-702.

449 [19] Lallemand B, Chaix F, Bury M, et al. N-(2-{3-[3, 5-bis (trifluoromethyl) phenyl]
450 ureido}ethyl)-glycyrrhetinamide(6b): a novel anticancer glycyrrhetinic acid derivative
451 that targets the proteasome and displays anti-kinase activity. *J. med. chem.* 2011,
452 54(19): 6501-6513.

453 [20] Sheldrick GM (1997) SHELXL 97. Program for the Refinement of Crystal
454 Structure, University of Go¨ttingen, Germany.

455 [21] Sheldrick GM (1997) SHELXS 97. Program for Crystal Structure
456 Determinations, University of Go¨ttingen, Germany.

[22] Wagstaff A J , Goa K L . Rosiglitazone. *Drugs*, 2002, 62(12):1805-1837.

[23] Ji C G , Zhang J Z H . Protein Polarization Is Critical to Stabilizing AF-2 and Helix-2′ Domains in Ligand Binding to PPAR-γ . *J Am Chem Soc*, 2008, 130(50):17129-17133.

[24] Lallemand B, Gelbcke M, Dubois J, et al. Structure-Activity Relationship Analyses of Glycyrrhetinic Acid Derivatives as Anticancer Agents. Mini-Rev Med Chem, 2011, 11(10):881-887.

479 **Table of Contents Graphic**

480

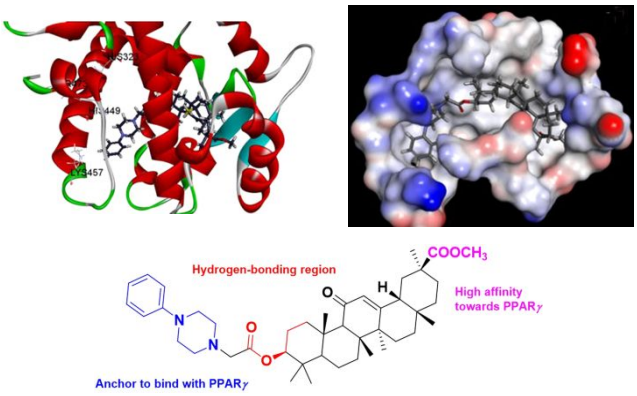

481